

IMPLICATIONS OF THE RADIO AFTERGLOW FROM THE GAMMA-RAY BURST OF 1997 MAY 8

E. WAXMAN

Institute for Advanced Study, Princeton, NJ 08540

S. R. KULKARNI

Division of Physics, Mathematics and Astronomy, 105-24, Caltech, Pasadena, CA 91125

AND

D. A. FRAIL

National Radio Astronomy Observatory, Socorro, NM 87801

Received 1997 September 19; accepted 1997 November 14

ABSTRACT

Radio observations of the afterglow of the γ -ray burst GRB 970508 provide unique new constraints on afterglow models. The quenching of diffractive scintillation at ~ 4 weeks delay provides the first direct estimate of source size and expansion rate. It implies an apparent size $R \sim 10^{17}$ cm and an expansion at a speed comparable to that of light at $t \sim 4$ weeks, in agreement with the fireball model prediction, $R = 10^{17}(t/\text{week})^{5/8}$ cm. The radio flux and its dependence on time and frequency at 1–5 weeks delay are in agreement with the model and imply a fireball energy (assuming spherical symmetry) $\sim 10^{52}$ ergs, consistent with the value inferred from observations at shorter delay. The observed radio behavior deviates from model predictions at delays greater than 5 weeks. This is expected, since at this delay the fireball is in transition from highly relativistic to subrelativistic expansion, with Lorentz factor $\gamma \leq 2$. Deviation may result from a change in the physical processes associated with the shock wave as it becomes subrelativistic (e.g., a decrease in the fraction of energy carried by the magnetic field) or from the fireball being a cone of opening angle $\sim 1/\gamma \sim \frac{1}{2}$. We predict the future behavior of the radio flux assuming that the latter interpretation is valid. These predictions may be tested by radio observations in the frequency range 0.1–10 GHz on a timescale of months.

Subject headings: gamma rays: bursts — radio continuum: general

1. INTRODUCTION

The availability of accurate positions for γ -ray bursts (GRBs) from the *BeppoSAX* satellite (Costa et al. 1997a; Feroci et al. 1997; Heise et al. 1997; Costa et al. 1997c) allowed, for the first time, the detection of delayed emission associated with GRBs in the X-ray (Costa et al. 1997a, 1997b; Feroci et al. 1997; Piro et al. 1997a, 1997b), optical (Groot et al. 1997; Sahu et al. 1997; van Paradijs et al. 1997; Bond 1997; Djorgovski et al. 1997), and radio (Frail & Kulkarni 1997) wave bands. The detection of absorption lines in the optical afterglow of GRB 970508 provided the first direct estimate of source distance, constraining the redshift of GRB 970508 to $0.86 < z < 2.3$ (Metzger et al. 1997). Observed X-ray to radio afterglow is most naturally explained by models based on relativistic blast waves at cosmological distances (Paczynski & Rhoads 1993; Mészáros & Rees 1997; Vietri 1997a; Waxman 1997a, 1997b; Wijers, Rees, & Mészáros 1997). Using these models, combined radio and optical data allowed, for the first time, the direct estimate of the total GRB energy, implying an energy of $\sim 10^{52}$ ergs (assuming spherical symmetry) for GRB 970508 (Waxman 1997b).

Radio observations of the afterglow of GRB 970508 (Frail et al. 1997; Taylor et al. 1997) provide unique new information on the afterglow source. Shortly after the first detection of the GRB radio afterglow, it was pointed out by Goodman (1997) that if the source angular size is as small as predicted by fireball models, $\sim 1 \mu$ as, then the radio flux should be modulated by scintillation caused by the local interstellar medium (ISM). The predicted modulation has been observed (Frail et al. 1997; Taylor et al. 1997), and it

provides the first direct constraints on source size and expansion rate. We discuss in § 3 the implications for fireball models of the observed modulation. In § 4 we discuss the implications for long-term afterglow behavior provided by the radio monitoring of GRB 970508 over 3 months. Deviation from model predictions is expected on this timescale (Waxman 1997b), as the fireball decelerates from highly relativistic to marginally relativistic speed. However, the lack of a theory describing the relevant physical processes associated with the shock wave (magnetic field generation, energy transfer to electrons) does not allow a unique interpretation of the observed behavior. We derive equations describing the fireball evolution in the nonrelativistic regime, which allow us to demonstrate that the observed behavior can not be accounted for by the deviation of the hydrodynamic evolution from that predicted by the highly relativistic scalings. We discuss possible interpretations of the long-term behavior and predict the future fireball radio emission under the assumption that the observed behavior results from a finite opening angle of the fireball. We summarize our conclusions and predictions in § 5.

We note here that two types of fireball models were considered in the literature as possible interpretations of the existing GRB 970508 afterglow data. In the “adiabatic” model (Waxman 1997b), the fireball radiates over time only a small fraction of its energy, which is of order 10^{52} ergs. In the “radiative” models (Vietri 1997b; Katz & Piran 1997) the fireball radiates most of its energy over a short time, and its energy is reduced to $\sim 10^{49}$ ergs on a timescale of days. We discuss in this paper mainly implications of radio observations for the adiabatic model, since, as we demonstrate in § 4, long-term radio observations rule out the radi-

ative models, and, as we briefly show in § 2, the radiative models are not self-consistent.

2. RADIATIVE VERSUS NONRADIATIVE MODELS

In fireball afterglow models, a highly relativistic shell encounters, after producing the GRB, some external medium. As the shell decelerates it drives a relativistic shock into the surrounding medium. This shock continuously heats fresh gas and accelerates relativistic electrons, which produce the observed radiation through synchrotron emission. The magnetic field B behind the shock and the characteristic Lorentz factor γ_e of the electrons are determined in these models by assuming that fractions ξ_e and ξ_B of the fireball energy are carried by electrons and the magnetic field, respectively. This implies $B^2/8\pi = 4\xi_B \gamma^2 n m_p c^2$ and $\gamma_e = \xi_e \gamma m_p/m_e$ (here, n is the number density of the surrounding medium, and γ is the fireball Lorentz factor). There is no theory that allows the determination of the values of ξ_e and ξ_B . Afterglow observations are consistent with $\xi_e \sim \xi_B \sim 0.1$ during the relativistic expansion of the fireball (Waxman 1997b).

The underlying assumption of radiative models is that all the kinetic energy lost by the fireball as it decelerates is radiated away. This requires an efficient process converting the kinetic energy flux to electron thermal energy, and it requires the electron cooling time to be much shorter than the dynamical time, i.e., the timescale for expansion in the fireball rest frame $\tau_d = r/4\gamma c$ (here, r is the fireball radius). The ratio of synchrotron cooling time $\tau_s = 6\pi m_e c/\sigma_T \gamma_e B^2$ to dynamical time is

$$\Theta \equiv \frac{\tau_s}{\tau_d} = \frac{3}{4} \left(\frac{m_e}{m_p} \right)^2 (\xi_e \xi_B \sigma_T n r \gamma^2)^{-1} = 16 \left(\frac{\xi_e \xi_B}{0.25} \right)^{-1} (n_1 r_{17} \gamma^2)^{-1}, \quad (1)$$

where $n = 1n_1 \text{ cm}^{-3}$, $r = 10^{17} r_{17} \text{ cm}$. (This result is similar to that given in Vietri 1997b.) In the radiative model of Katz & Piran (1997), the fireball expands into a uniform-density medium, $n_1 = 1$, and because of rapid energy loss, the fireball becomes nonrelativistic at a 6 day delay with $r_{17} \sim \gamma \sim 1$. In the radiative model of Vietri (1997b), the ambient-medium density drops with radius as r^{-2} , allowing the fireball to remain relativistic as it loses energy. In this case $n_1 \sim 10^{-3}$ and $r_{17} \sim \gamma \sim 3$ at $t = 6$ days. In both models, therefore, $\Theta \gg 1$ at this time. Furthermore, the time dependence of Θ , $\Theta \propto t^1$ for $n \propto r^{-2}$ and $\Theta \propto t^{5/7}$ for uniform density, implies that the assumption that $\Theta \ll 1$ is not valid in both models for $t \gtrsim 1 \text{ hr}$.

3. SOURCE SIZE AND EXPANSION RATE

Due to relativistic beaming, the radiation from a relativistic fireball seen by a distant observer is emitted from a cone of the fireball around the source-observer line of sight with an opening angle $\sim 1/\gamma$. The apparent radius of the emitting cone is $R = r/\gamma$, where r is the fireball radius, and photons emitted from such a cone are delayed, compared to those emitted on the line of sight, by $t = r/2\gamma^2 c$. Thus, the apparent radius of the fireball is $R = 2\gamma(r)ct$ [a detailed calculation of fireball emission (Waxman 1997c) introduces only a small correction, $R = 1.9\gamma(r)ct$], where r and t are related by $t = r/2\gamma^2 c$. Using equations (1) and (2) of

Waxman (1997b) we have

$$\gamma = 4 \left(\frac{1+z}{2} \right)^{3/8} \left(\frac{E_{52}}{n_1} \right)^{1/8} t_w^{-3/8}, \quad (2)$$

and

$$R = 8 \times 10^{16} \left(\frac{1+z}{2} \right)^{-5/8} \left(\frac{E_{52}}{n_1} \right)^{1/8} t_w^{5/8} \text{ cm}. \quad (3)$$

Here, $E = 10^{52} E_{52} \text{ ergs}$ is the fireball energy and $t = 1t_w$ weeks. (Note that the relation $t = r/2\gamma^2 c$ should not be replaced by $t = r/16\gamma^2 c$, as recently argued in Sari 1997, since the latter relation holds only for the arrival time of photons that are emitted on the line of sight and is not valid for most of the photons, which are emitted from a cone of opening angle $\sim 1/\gamma$ [Waxman 1997c].)

Scattering by irregularities in the local ISM may modulate the observed fireball radio flux (Goodman 1997). If scattering produces multiple images of the source, interference between the multiple images may produce a diffraction pattern (on an imaginary plane perpendicular to the line of sight), leading to strong variations of the flux as the observer moves through the pattern. Two conditions need to be met in order for such diffractive scintillation to be produced: (i) The scattering should be strong enough to produce multiple images. (ii) The source size should be small enough that different points on the source produce similar diffraction patterns. There is significant observational evidence that ISM electron density fluctuations are described by a power-law spectrum, $\langle \delta N_e(k) \delta N_e(-k) \rangle = C_N^2 k^{-11/3}$, where k is the spatial wavenumber. For this distribution, the characteristic deflection angle is given by $\theta_d = 2.34 \lambda^{11/5} r_e^{6/5} (\text{SM})^{3/5}$, where λ is the wavelength, r_e the classical electron radius, and the scattering measure SM is the integral of C_N^2 along the line of sight. In the framework of the “thin screen” approximation, i.e., assuming that all scattering occurs in a narrow layer at distance d_{sc} , multiple images are produced for frequencies (Goodman 1997):

$$\nu \lesssim 11 d_{\text{sc}, \text{kpc}}^{6/17} \left(\frac{\text{SM}}{10^{-3.5} \text{ m}^{-20/3} \text{ kpc}} \right)^{5/17} \text{ GHz}. \quad (4)$$

Here, values were chosen for the ISM scattering properties SM and d_{sc} that are typical for sources at high Galactic latitude ($b = 27^\circ$ for GRB 970508). The characteristic length scale of the diffraction pattern is

$$dx = \frac{\lambda}{2\pi\theta_d} = 3.3 \times 10^{10} \nu_{10}^{6/5} \left(\frac{\text{SM}}{10^{-3.5} \text{ m}^{-20/3} \text{ kpc}} \right)^{-3/5} \text{ cm}. \quad (5)$$

In order for the diffraction patterns produced by different points on the source to be similar, so that the pattern is not smoothed out because of large source size, the angular source size θ_s should satisfy $\theta_s d_{\text{sc}} < dx$. For a source at redshift $z = 1$, this requirement implies an upper limit to the apparent source size

$$R < 1.0 \times 10^{17} \frac{\nu_{10}^{6/5}}{d_{\text{sc}, \text{kpc}} h_{75}} \left(\frac{\text{SM}}{10^{-3.5} \text{ m}^{-20/3} \text{ kpc}} \right)^{-3/5} \text{ cm}, \quad (6)$$

where $\nu = 10\nu_{10} \text{ GHz}$, h_{75} is the Hubble constant in units of $75 \text{ km s}^{-1} \text{ Mpc}^{-1}$. Due to the weak dependence of the angular diameter distance on z , the upper limit on R is not sensitive to source redshift. The main uncertainty in (6) is

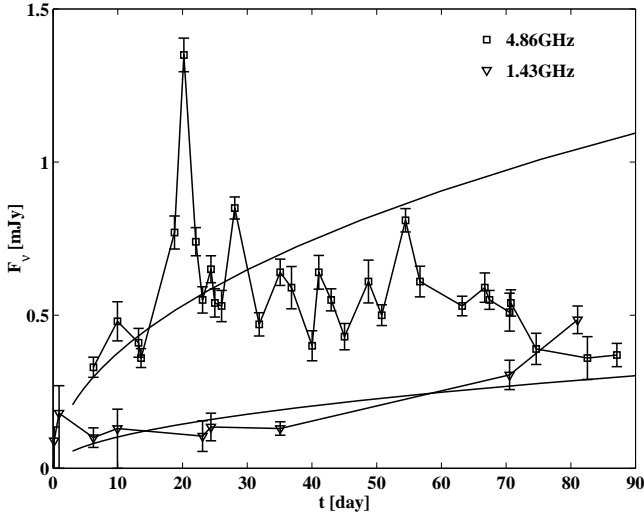


FIG. 1a

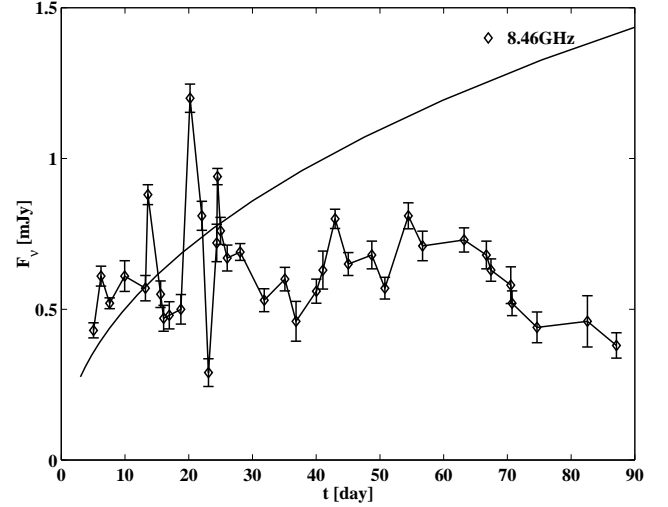


FIG. 1b

FIG. 1.—(a) Light curves of the radio afterglow of GRB 970508 at 4.86 and 1.43 GHz, compared to the predictions of the adiabatic fireball model (Waxman 1997b). (b) Light curve of the radio afterglow of GRB 970508 at 8.46 GHz, compared to fireball model predictions (Waxman 1997b).

caused by uncertainty in the scattering properties of the ISM. Combining (6) and (4), we find that

$$R < 1.1 \times 10^{17} d_{\text{sc,kpc}}^{-11/17} h_{75}^{-1} \left(\frac{\text{SM}}{10^{-3.5} \text{ m}^{-20/3} \text{ kpc}} \right)^{-3/17} \text{ cm} \quad (7)$$

is required to allow diffractive scintillation. Due to variations in ISM scattering properties along different lines of sight, the numerical value in (7) is accurate to a factor of a few.

The frequency range $\Delta\nu$ over which the diffraction pattern is similar, and therefore over which flux modulation is correlated, is

$$\Delta\nu = \frac{c}{2\pi\theta_d^2 d_{\text{sc}}} = 0.4 d_{\text{sc,kpc}}^{-1} \left(\frac{\text{SM}}{10^{-3.5} \text{ m}^{-20/3} \text{ kpc}} \right)^{-6/5} \times \left(\frac{\nu}{5 \text{ GHz}} \right)^{22/5} \text{ GHz}. \quad (8)$$

For a characteristic velocity through the diffraction pattern of $\simeq 30 \text{ km s}^{-1}$, due to Earth's orbital motion and to the Sun's peculiar velocity, equation (5) implies a timescale for variations of $\simeq 3 \text{ hr}$.

Comparing equation (3) and requirement (7), we find that on a timescale of weeks the apparent fireball size is comparable to the maximum size for which diffractive scintillation is possible. On shorter timescales, therefore, strong modulation of the radio flux is expected. On longer timescales we expect diffractive scintillation to be quenched as a result of large source size. When diffractive scintillation is quenched, the flux is nevertheless expected to be modulated because of refraction (i.e., due to focusing/defocusing of rays). However, the modulation amplitude should decrease (to $\sim 10\%$; Goodman 1997), and modulation should be correlated over a wide frequency range. Figure 1 presents the light curves of the radio afterglow at 8.46, 4.86, and 1.43 GHz. Figure 2 presents the fluxes at 4.86 GHz as a function of the flux at 8.46 GHz. Strong modulation of the radio flux is observed during the first month, accompanied by strong variations in the ratio of flux at 8.46 and 4.86 GHz. This

behavior is consistent with that expected as a result of diffractive scintillation. The radio flux is not sampled at a sufficient rate to determine whether the variability timescale is consistent with that expected for diffractive scintillation. At delays longer than ~ 1 month, the modulation amplitude decreases, and the flux ratio is consistent with being constant. This is consistent with the quenching of diffractive scintillation as a result of increased source size.

Observations are therefore in agreement with fireball model predictions. They imply that the source size is close to the upper limit given by equation (7) after ~ 1 month. This is consistent with equation (3) and implies expansion at

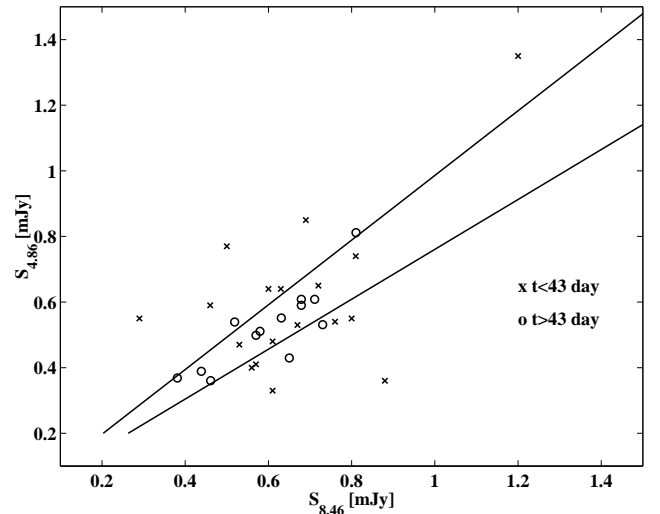


FIG. 2.—Flux at 4.86 GHz as a function of the flux at 8.46 GHz for $t > 43$ days and $t < 43$ days (first/second half of observing time). The average value of the flux ratio $f \equiv S_{8.46}/S_{4.86}$ for $t > 43$ days is $\bar{f} = 1.17$, and the standard deviation in f is $\sigma = 0.15$ (solid lines, border of region of 1σ). The scatter is consistent with that expected from errors in flux measurement ($\chi^2 = 17.6$ for the hypothesis that $f = \bar{f}$ for the 13 data points), and \bar{f} is consistent with the value expected in the fireball model, $f = (8.46/4.86)^{1/3} = 1.20$. At delays $t < 43$ days, the average flux ratio is similar: $\bar{f} = 1.18$. The scatter, however, is large ($\sigma = 0.45$) and inconsistent with that expected from measurement errors ($\chi^2 = 267$ for the hypothesis that $f = \bar{f}$ for the 18 data points).

a speed comparable to that of light. Due to the very weak dependence of R on fireball model parameters, it is not possible to determine parameters based on the quenching of diffractive scintillation accurately. On the other hand, since R is very insensitive to model parameters, reducing the uncertainty in the size estimate based on scintillation by reducing the uncertainty in ISM scattering properties toward the GRB would provide a stringent test of the fireball model.

4. LONG-TERM BEHAVIOR

4.1. Relativistic Regime

The radio light curves are compared to the predictions of the adiabatic fireball model (Waxman 1997b) in Figure 1. In this model, the observed frequency at which the synchrotron spectral intensity peaks is

$$\nu_m^R = 5 \times 10^{12} \left(\frac{1+z}{2} \right)^{1/2} \left(\frac{\xi_e}{0.2} \right)^2 \left(\frac{\xi_B}{0.1} \right)^{1/2} E_{52}^{1/2} t_w^{-3/2} \text{ Hz}, \quad (9)$$

and the observed intensity at ν_m is

$$F_{\nu_m}^R = 1 \left(\frac{1+z}{2} \right)^{-1} \left(\frac{1 - 1/\sqrt{2}}{1 - 1/\sqrt{1+z}} \right)^2 n_1^{1/2} \left(\frac{\xi_B}{0.1} \right)^{1/2} E_{52} \text{ mJy}. \quad (10)$$

The superscript R implies that the expressions are valid for the highly relativistic regime. The flux at ν_m is produced by electrons at the characteristic electron energy $\varepsilon = \gamma_e m_e c^2$. The flux at higher frequency is produced by higher energy electrons. For a power-law electron spectrum, $dN_e/d\varepsilon \propto \varepsilon_e^{-p}$, $F_\nu \propto \nu^{-(p-1)/2}$ at $\nu > \nu_m$. Typical parameters required to fit observations are $E_{52} \sim n_1 \sim 1$, $\xi_e \sim \xi_B \sim 0.1$, and $p \sim 2$.

The flux at low frequency $\nu < \nu_m$ is due to the extension of synchrotron emission of electrons at $\varepsilon = \gamma_e m_e c^2$ to frequencies $\nu < \nu_m$ [$F_\nu \propto (\nu/\nu_m)^{1/3}$ at $\nu \ll \nu_m$]. At low frequency self-absorption becomes significant. The self-absorption frequency, where the fireball optical depth is unity, is

$$\nu_A^R = 1 \left(\frac{1+z}{2} \right)^{-1} \left(\frac{\xi_e}{0.2} \right)^{-1} \left(\frac{\xi_B}{0.1} \right)^{1/5} E_{52}^{1/5} n_1^{3/5} \text{ GHz}, \quad (11)$$

and at $\nu < \nu_m$, the optical depth is given by $\tau_\nu = (\nu/\nu_A)^{-5/3}$. Self-absorption reduces the flux by a factor $(1 - e^{-\tau_\nu})/\tau_\nu$.

The solid smooth curves in Figure 1 give the model fluxes for $E_{52} = n_1 = 2$, $\xi_e = 0.2$, and $\xi_B = 0.1$. These are essentially the same parameter values inferred in Waxman (1997b) from optical and radio afterglow data at delays $t \leq 6$ days. Although many simplifying assumptions were made, in order to obtain a simple description of fireball behavior, the model is in agreement with the data obtained during the first ~ 5 weeks. At later times model curves deviate from the data. This behavior is expected (Waxman 1997b), as the fireball decelerates from highly relativistic to marginally relativistic speed. At this stage the scalings (2) and (3) do not give an accurate description of the fireball dynamics. Furthermore, there is no theory that allows us to determine the parameters ξ_e and ξ_B . These parameters may change as the shock decelerates, thus affecting the predictions of equations (9)–(11). Before discussing (§ 5) the possible implications of observations at $t > 5$ weeks, we derive in § 4.2 the equations describing the fireball dynamics at the

nonrelativistic stage. This would allow us to estimate the effects of deviation from the scaling laws (eqs. [2] and [3]).

4.2. Transition to the Nonrelativistic Regime

As the fireball becomes nonrelativistic, its expansion approaches that described by the Sedov–von Neumann–Taylor solutions (Sedov 1946; von Neumann 1947; Taylor 1950). At this stage the shock radius is given by $r = \xi_0(\hat{\gamma})(Et^2/nm_p c^2)^{1/5}$, where ξ_0 is a function of the adiabatic index of the gas $\hat{\gamma}$. $\xi_0 = 0.99$ for $\hat{\gamma} = 4/3$ (relativistic fluid), and $\xi_0 = 1.15$ for $\hat{\gamma} = 5/3$ (nonrelativistic limit). The nonrelativistic behavior may be described as

$$\beta \equiv \dot{r}/c = \xi_0^{5/2} (r/r_{\text{NR}})^{-3/2}, \quad r/r_{\text{NR}} = (\xi_0/1.15)(t/t_{\text{NR}})^{2/5}, \quad (12)$$

by defining

$$r_{\text{NR}} = 1.0 \times 10^{18} \left(\frac{E_{52}}{n_1} \right)^{1/3} \text{ cm},$$

$$t_{\text{NR}} = 24 \frac{1+z}{2} \left(\frac{E_{52}}{n_1} \right)^{1/3} \text{ weeks}. \quad (13)$$

With these definitions, the time dependence (eq. [2]) of the Lorentz factor in the highly relativistic regime may be written as $\gamma = 1.3(t/t_{\text{NR}})^{-3/8}$. Thus, the relativistic solution is valid for $t \ll t_{\text{NR}}$, where $\gamma^2 \gg 1$, and the nonrelativistic solution for $t \gg t_{\text{NR}}$, where $\beta^2 \ll 1$.

For the nonrelativistic regime, assuming that fractions ξ_B and ξ_e of the dissipated energy are carried by magnetic field and electrons implies $B^2/8\pi = \beta^2 n m_p c^2$, and characteristic electron Lorentz factor $\gamma_e = (m_p/2m_e)\xi_e \beta^2$. The frequency at which the synchrotron intensity peaks, $\nu_m = \gamma_e^2 eB/2\pi m_e c$, is

$$\nu_m^{\text{NR}} = 4 \left(\frac{1+z}{2} \right)^{-1} \left(\frac{\xi_e}{0.2} \right)^2 \left(\frac{\xi_B}{0.1} \right)^{1/2} n_1 \beta^5 \text{ GHz}. \quad (14)$$

The intensity at ν_m is $F_{\nu_m}^{\text{NR}} = N_e (3^{1/2} e^3 B/2\pi m_e c^2) (1+z)/4\pi d_L^2$, where $N_e = 4\pi r^3 n/3$ is the number of radiating electrons, and d_L is the luminosity distance. Using equation (10), we have

$$F_{\nu_m}^{\text{NR}} = F_{\nu_m}^R \beta \left(\frac{r}{r_{\text{NR}}} \right)^3. \quad (15)$$

Extrapolation of the nonrelativistic equation (15) to $t = t_{\text{NR}}$ gives a peak flux that is similar to that given by equation (10) for the relativistic regime. This is expected, since in the relativistic regime, F_{ν_m} is independent of time, and therefore of γ . Thus, as the fireball decelerates to nonrelativistic speed, the peak flux is approximately given by the relativistic equation (10). At later time, $t \gg t_{\text{NR}}$, and $F_{\nu_m} \propto (t/t_{\text{NR}})^{3/5}$. Extrapolation of the relativistic expression (9) for ν_m to $t = t_{\text{NR}}$ gives $\nu_m = 100(\xi_e/0.2)^2(\xi_B/0.1)^{1/2} n_1^{1/2} \text{ GHz}$, which is significantly higher than the extrapolation of the nonrelativistic expression (14). Thus, as the fireball decelerates, ν_m decreases with time faster than given by equation (9), and $\nu_m \propto (t/t_{\text{NR}})^{-3}$ for $t \gg t_{\text{NR}}$.

The self-absorption frequency where the fireball optical depth is unity is

$$\nu_A^{\text{NR}} = \nu_A^R \beta^{-8/5} \left(\frac{r}{r_{\text{NR}}} \right)^{3/5}. \quad (16)$$

Comparing equations (16) and (11), we find that the self-absorption frequency is time independent and is given by the relativistic expression for $t < t_{\text{NR}}$. At a later time, equation (16) implies that the self-absorption frequency

increases. However, equation (16) is valid only as long as $v_A < v_m$. Since the dependence of v_m on time for $t > t_{\text{NR}}$ is stronger than that of v_A , v_m drops below v_A when v_A is not significantly higher than the value given by equation (11). At a later time, v_A decreases with time. For an electron spectrum $dN_e/d\varepsilon_e \propto \varepsilon_e^{-2}$, $v_A \propto (t/t_{\text{NR}})^{-2/3}$.

5. IMPLICATIONS

5.1. Ruling out Radiative Expansion

From the analysis of § 4.2, the relativistic expression (10) is a good approximation for the fireball peak flux, not only for $\gamma \gg 1$, but as long as $\beta \sim 1$. Since radio observations imply that the fireball expands with $\beta \sim 1$ on a timescale of weeks, the observed flux of order 1 mJy implies that $E_{52} n_1^{1/2} \gtrsim 1$ on a timescale of weeks. This rules out the radiative models, in which the fireball energy decreases to 10^{49} ergs on a timescale of days. We note here that it was argued in Katz & Piran (1997) that a mildly relativistic fireball, $\gamma - 1 \sim 1$, with $E \sim 10^{49}$ ergs, would produce the observed ~ 0.1 mJy flux at 1.43 GHz at a ~ 6 day delay. This is in contradiction with our results, equations (10) and (15), which imply a much lower flux. The Katz & Piran (1997) derivation is, however, not self-consistent. The flux at 1.43 GHz is obtained in Katz & Piran (1997) using the Rayleigh-Jeans law, for which $F_\nu \propto \nu^2$, and which is valid only for high optical depth. From equations (11) and (16), the self-absorption frequency for the parameters chosen in Katz & Piran (1997), $E \sim 10^{49}$ ergs and $n_1 = 1$, is $\simeq 0.2$ GHz. Using the Rayleigh-Jeans formula for the flux at 1.43 GHz, where $\tau_\nu \simeq 0.05$, overestimates the flux by a factor $(1 - e^{-\tau_\nu})^{-1} \sim 30$.

5.2. Deviations during the Transition to Nonrelativistic Expansion

On a timescale $\gtrsim 5$ weeks, the observed radio behavior deviates from model predictions. The flux at 4.86 and 8.46 GHz is significantly below model predictions at $t \sim 10$ weeks. The increase of flux at 1.43 GHz at this time indicates that the frequency ν_m at which the intensity peaks drops to ~ 5 GHz at $t \sim 10$ weeks, for which equation (9) predicts $\nu_m \sim 100$ GHz. From the analysis of § 5.1, this behavior can not be explained based only on the deviation from the highly relativistic scaling laws (2) and (3), as the fireball decelerates to mildly relativistic velocity, $\gamma - 1 \sim 1$. The synchrotron peak intensity is not expected to decrease (cf. eq. [15]), and therefore the decrease in the 4.86 and 8.46 GHz flux can not be accounted for. The peak frequency ν_m is expected to decrease faster than predicted by equation (9). However, it is expected to decrease to ~ 5 GHz only when the fireball becomes nonrelativistic, i.e., at $t \sim t_{\text{NR}} \sim 24$ weeks (cf. eqs. [14] and [12]). Note that a change in the ambient medium density n is not likely to account for the observed behavior. A decrease in flux may result from a decrease in n (eq. [10]). However, the peak frequency (eq. [9]) is independent of n , and the apparent decrease in ν_m can not be accounted for.

Clearly, the observed behavior may be explained by deviations of the equipartition fractions ξ_e and ξ_B from the values $\xi_e \sim \xi_B \sim 0.1$, which are implied by observations at $t < 5$ weeks. Due to the lack of a theory determining these parameters, it is not possible to predict their dependence on shock Lorentz factor. Thus, if the observed behavior is due to changes in ξ_e and ξ_B , it is difficult to predict the future

fireball behavior. However, the observed deviations from the model may also result from a different effect. This is discussed below.

5.3. Nonspherical Fireballs

We have thus far assumed that the fireball is spherically symmetric. The results are valid also for the case in which the fireball is a cone of finite opening angle θ , as long as $\gamma > 1/\theta$. In this case, the fireball energy E in the equations should be understood as the energy the fireball would have had if it were spherically symmetric. The actual fireball energy is $E' \simeq \theta^2 E/2$. Deviations from the spherical model would appear at a late time as γ decreases below $1/\theta$ and the fireball starts expanding transversely as well as radially. Let us briefly discuss the expected behavior at a later time.

After a transition phase the fireball would approach spherically symmetric expansion, which may again be described by the equations derived above, with E replaced by the actual fireball energy E' . Numerical calculations would probably be required to describe the fireball evolution in the stage at which it approaches spherically symmetric behavior. Qualitatively, as the fireball expands transversely, its energy per unit solid angle along the line of sight decreases. Thus, it would appear as if the fireball energy is decreasing with time. This would lead to decrease in the peak flux (cf. eq. [10]) and in the peak frequency (cf. eq. [9]), in qualitative agreement with the observed trends. The timescale for transition to spherically symmetric behavior may be estimated as follows. The scaling laws (2) are derived from energy conservation, $E \simeq \gamma^2 (4\pi r^3/3) n m_p c^2$. This implies that at the radius r_θ , where $\gamma = 1/\theta$, the rest-mass energy contained in the sphere with $r = r_\theta$ is comparable to the total fireball energy E' . Thus, as the fireball approaches spherically symmetric behavior, it necessarily becomes subrelativistic, and at later times it is described by equations (14)–(16), with E replaced by E' . The transition to spherical nonrelativistic behavior occurs on a timescale (cf. eq. [13]) $t_{\text{NR}} = 18(\theta^2 E_{52}/n_1)^{1/3}$ weeks.

The deviation at $t \sim 5$ weeks from model predictions may therefore be accounted for by the fireball being a cone of opening angle $\theta \sim 1/\gamma(5 \text{ week}) \sim \frac{1}{2}$. This implies that the “real” fireball energy is $E' \sim 2 \times 10^{51}$ ergs. In this case, the decrease in flux and in peak frequency are accounted for by the transition to spherical nonrelativistic behavior. The transition should take place on a timescale $t_{\text{NR}} \sim 12$ weeks. On this timescale the peak frequency is expected to decrease to ~ 4 GHz (cf. eq. [14]) and the peak intensity to ~ 0.3 mJy (cf. eq. [15]). This is in agreement with the observed behavior. The fireball behavior for $t \gg 12$ weeks is described by equations (12)–(16), with $E_{52} \simeq 0.2$, $n_1 = 2$.

6. CONCLUSIONS

Comparison of radio observations of the afterglow of the γ -ray burst GRB 970508 with fireball model predictions lead to the following conclusions:

1. The source size implied by the quenching of diffractive scintillation at ~ 4 weeks, $\sim 10^{17}$ cm, and the inferred expansion at a speed comparable to that of light are consistent with published (Waxman 1997b) model predictions, equations (2) and (3).

2. The radio flux and its dependence on time and frequency at a 1–5 week delay are in agreement with the model (Fig. 1) and imply a fireball energy (assuming spherical

symmetry) $\sim 10^{52}$ ergs. This is consistent with the value inferred from observations at shorter delay (Waxman 1997b) and rules out “radiative” models (Vietri 1997b; Katz & Piran 1997), where fireball energy is reduced to $\sim 10^{49}$ ergs on a day timescale.

3. The deviation of observed radio behavior from model predictions at delays greater than 4 weeks is expected, as on this timescale the fireball is in transition from highly relativistic to subrelativistic expansion, with Lorentz factor $\gamma \leq 2$. We have shown that the observed behavior can not be accounted for by the deviation of the hydrodynamic behavior from that predicted by the highly relativistic scalings (2) and (3) or by changes in ambient medium density.

4. The observed behavior may be explained by the deviation of the equipartition fractions ξ_e and ξ_B from the values $\xi_e \sim \xi_B \sim 0.1$, which are implied by observations at $t < 5$ weeks. Due to the lack of a theory determining these parameters, it is not possible to predict their dependence on shock Lorentz factor. Thus, if the observed behavior is due to changes in ξ_e and ξ_B , it is difficult to predict the future fireball behavior.

5. However, the observed behavior at $t > 5$ weeks may also be accounted for by the fireball being a cone of finite opening angle $\theta \sim 1/\gamma(5 \text{ weeks}) \sim \frac{1}{2}$, which implies that the “real” fireball energy is $E' \simeq \theta^2 E/2 \sim 2 \times 10^{51}$ ergs. In this case, at $t \sim 5$ weeks the fireball rapidly expands transversely, leading to a decrease in the energy per solid angle along the line of sight. This may account for the observed decrease in peak flux and peak frequency. On a timescale $t_{\text{NR}} \sim 12$ weeks (cf. eq. [13]), the fireball approaches spherical nonrelativistic expansion. On this timescale the peak frequency is expected to decrease to ~ 4 GHz (cf. eq. [14])

and the peak intensity to ~ 0.3 mJy (cf. eq. [15]). This is in agreement with the observed behavior.

If the observed behavior is indeed due to the fireball being a cone of finite opening angle, then the future behavior may be predicted. On a timescale of ~ 12 weeks, the fireball should approach spherical nonrelativistic expansion. At times $t \gg 12$ weeks, the behavior is given by equations (12)–(16), which describe the spherical nonrelativistic behavior, with $E_{52} \simeq 0.2$, $n_1 = 2$. The frequency at which the intensity peaks should decrease with time $\nu_m \propto t^{-3}$, dropping to 0.3 GHz in ~ 0.5 yr. The peak intensity should be ~ 0.3 mJy over this period. If the electron energy distribution is similar to the distribution inferred for the relativistic regime, $dN_e/d\varepsilon_e \propto \varepsilon_e^{-p}$ with $p \sim 2$, then the flux at $\nu > \nu_m$ should decrease approximately as t^{-1} , similar to the highly relativistic case, and at a given time the intensity should drop with frequency as $\nu^{-\alpha}$ with $\alpha \sim 0.5$.

The time dependence of the flux at $\nu > \nu_m$ is similar in the nonrelativistic and the relativistic regimes. At early times, $t < 1$ weeks, the optical flux decrease as t^{-1} (Djorgovski et al. 1997). However, the optical flux should drop, at ~ 5 weeks, below the t^{-1} extrapolation from early time, as the effective fireball energy decreases. The flux expected at ~ 10 weeks in this model is $m_R \sim 25$. Agreement of the observed optical behavior with the behavior described above would provide support for the model discussed here, where it is assumed that both optical and radio fluxes are produced by the expanding fireball.

E. W. acknowledges support from a W. M. Keck Foundation grant and NSF grant PHY 95-13835.

REFERENCES

- Bond, H. E. 1997, IAU Circ. 6654
 Costa, E., et al. 1997a, IAU Circ. 6572
 ———. 1997b, IAU Circ. 6576
 ———. 1997c, IAU Circ. 6649
 Djorgovski, S. G., et al. 1997, *Nature*, 387, 876
 Feroci, M., et al. 1997, IAU Circ. 6610
 Frail, D. A., & Kulkarni, S. R. 1997, IAU Circ. 6662
 Frail, D. A., Kulkarni, S. R., Nicastro, L., Feroci, M., & Taylor, G. B. 1997, *Nature*, 389, 261
 Goodman, J. 1997, *New Astron.*, 2, 449
 Groot, P. J., et al. 1997, IAU Circ. 6584
 Heise, J., et al. 1997, IAU Circ. 6610
 Katz, J. I., & Piran, T. 1997, *ApJ*, 490, 772
 Mészáros, P., & Rees, M. 1997, *ApJ*, 476, 232
 Metzger, M. R., et al. 1997, IAU Circ. 6655
 Paczyński, B., & Rhoads, J. 1993, *ApJ*, 418, L5
 Piro, L., et al. 1997a, IAU Circ. 6617
 ———. 1997b, IAU Circ. 6656
 Sahu, K., et al. 1997, IAU Circ. 6619
 Sari, R. 1997, *ApJ*, submitted
 Sedov, L. I. 1946, *Prikl. Mat. i Mekh.*, 10, 241
 Taylor, G. B., Frail, D. A., Beasley, A. J., & Kulkarni, S. R. 1997, *Nature*, 389, 263
 Taylor, G. I. 1950, *Proc. R. Soc. London A*, 201, 159
 van Paradijs, J., et al. 1997, *Nature*, 386, 686
 von Neumann, J. 1947, *Los Alamos Sci. Lab. Tech. Series*, 7
 Vietri, M. 1997a, *ApJ*, 478, L9
 ———. 1997b, *ApJ*, submitted
 Waxman, E. 1997a, *ApJ*, 485, L5
 ———. 1997b, *ApJ*, 489, L33
 ———. 1997c, *ApJ*, 491, L19
 Wijers, A. M. J., Rees, M. J., & Mészáros, P. 1997, *MNRAS*, 288, L51